ELSEVIER

Biophysical Chemistry 56 (1995) 227–239

Biophysical Chemistry

Diffusion influenced binary reactive processes in membranes involving identical particles: a Monte Carlo study

Sebastian Bergling *

Biocenter of the University of Basel, Klingelbergstr. 70, CH-4056 Basel, Switzerland [1]

Received 24 October 1994; accepted 15 February 1995

Abstract

Simple random walk simulations on triangular lattices were performed in order to obtain a basic quantitative understanding of the kinetics of diffusion influenced binary reactive processes of membrane associated peptides or proteins within the two dimensionality of lipid bilayers. The results of the Monte Carlo simulations are compared with various formal approximate steady-state approaches, such as presented by Keizer [Acc. Chem. Res., 18 (1985) 235–241] in the context of statistical nonequilibrium thermodynamics or by Hardt [Biophys. Chem., 10 (1979) 239–243], based on the well known work of Delbrück and Adam. For diffusion controlled binary reactions of identical particles, nice agreement with the numerically simulated values is found in the low concentration limit for both Hardt's and Keizer's approach. For the latter a fluctuating steady-state particle source has to be considered. The dependence of the steady-state rate coefficient on system size is investigated, and the results are compared to the work of Swartz and Peacock-López [J. Chem. Phys., 95 (4) (1991) 2727–2731]. In order to elucidate the results, a practical application is considered. An application to a dimerization reaction on vesicles of typical experimental dimensions is given.

Keywords: Random walk; Monte Carlo simulation; Diffusion controlled reactions; Lipid bilayer; Monolayers; Unilamellar vesicles

1. Introduction

In 1972 Singer and Nicolson proposed their fluid mosaic model of biological membranes [1]. It is now well accepted that with few exceptions the lipid bilayers of biological membranes can be regarded as 2-d fluid systems in which membrane proteins can diffuse freely in the plane of the bilayer. Recently it became clear that the lateral diffusion of membrane active substances in biomembranes might be strongly influenced by obstacles such as membrane proteins ([2–4] and refs. therein). Delbrück and Adam explored in an important publication [5] the consequences of reduced dimensionality for biological systems: they showed that in the limit of DC reactions and for the small geometrical extension of living cells a combination of 2-d and 3-d diffusion can

Abbreviations: RW: random walk; DC: diffusion controlled; n-d: n-dimensional; MC: Monte Carlo; SUV: small unilamellar vesicles; MCS: Monte Carlo step

* Corresponding author.

[1] Current address: Institute of Theoretical Dynamics, UC Davis, Davis, CA 95616, USA.

SSDI 0301-4622(95)00037-2

enhance reaction rates compared to the purely 3-d diffusion.

Processes confined in the two dimensionality of biological membranes play an important role in the living cell. The following examples should illustrate this fact. Many enzymes and proteins that are essential in signal transduction pathways interact while confined to the plasma membrane. Similarly, the electron transport chain of cytochrome *c* and their redox partners, some of which are integral membrane proteins located in the mitochondrial inner membrane, are involved in partially DC 2-d electron transfer reactions. Gupte, Hackenbrock, and associates [6,7] have described this using the theoretical approach of Hardt [8]. Receptor mediated endocytosis provides another example. After binding to the receptor, the ligand receptor complex moves laterally by diffusion in the plane of the plasma membrane until it encounters specialized patches able to form coated pits. At these coated pits the plasma membrane is able to invaginate, leading to endocytosis. Peacock-López and coworkers [9–11] have used a statistical theory based on nonequilibrium thermodynamics [12,13] to analyse the steady state of receptor mediated endocytosis.

The work reported here was stimulated by the experiments of Schwarz and colleagues who have been investigating the kinetics and thermodynamics of pore forming peptides, e.g., the antibiotic alamethicin and insect venom components such as melittin and mastoporan [14–17].

For a quantitative understanding of such processes, the effect of diffusion on reactive processes in two dimensions must be examined. The role of lateral diffusion and possible diffusion coupled mechanisms of membrane associated peptides in the kinetics of pore forming are not fully understood. Because of this and the varying sizes of liposomes, organelles, and cells, it is of general interest to analyse DC 2-d reactive systems and the influence of the system size of closed membranes. In addition to the approaches of Keizer [13] and Hardt [8], Clément et al. [18] have developed a master equation approach for DC binary reactive 2-d systems in the steady-state regime. As the three approaches lead to different results, random walk simulations are used here to check the range of validity of the different approaches.

2. Theory and computation

2.1. Assumptions and conventions

For the discussion of 2-d DC reactive processes in the following sections, we should bear in mind that the various models discussed are of course idealizations of possible reactive events restricted to the plane of biomembranes (or monolayers). All simulations are based on the following assumptions:

(1) The 3-d structure of lipid bilayers is restricted to its 2-d extension, determined by the plane of the membrane.
(2) The membrane associated reactive particles are assumed to be circular when their 3-d shape is projected to the plane of the membrane.
(3) Although the association state of the particles under consideration might be membrane spanning, inserted in one monolayer only, or adsorbed to the membrane surface, their lateral diffusion is characterized by a single diffusion coefficient, D, and the particles meet each other in the plane of the membrane.
(4) The lipid bilayer does not contain obstacles that influence the long range diffusion of the reactive particles [2].
(5) The bilayer is a liquid continuum.

The idealized reactive particle is meant to represent an uncharged peptide, about 20 to 25 amino-residues long. In its membrane associated state it has an α-helical structure. The peptide is membrane spanning with its symmetry axis perpendicular to the plane of the membrane. In this state the peptide can be approximated by a cylinder of about 1 nm diameter and a length in the range of 3 nm to 4 nm as shown in Fig. 1. The antibiotic alamethicin in its neutral form, for example, matches these requirements ([14] and refs. therein). In its 2-d projection the size of the peptide corresponds to an encounter radius of about 1 nm. Throughout this text we will often use this example as a point of reference.

We consider second order reactions of the kind

$$A + A \rightarrow P \qquad (1)$$

The reaction rate V^+ is expressed as the number of product particles, P, formed per area per time. It defines by

$$V^+ = k^+ \rho_A^2$$

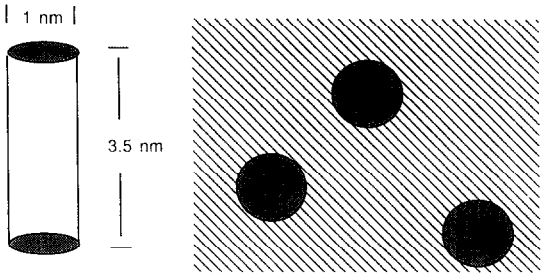

Fig. 1. Sketch of a membrane spanning peptide in an α-helical conformation approximated by a cylinder with size as indicated. In 2-d the peptide is approximated by a circle of 1 nm diameter, which corresponds to an encounter radius of $R_{enc} = 1$ nm.

a coefficient, k^+, which we refer to as the 'reaction rate coefficient'. For DC 2-d reactive systems, K^+ depends on the reaction concentration, ρ_A, as will be seen below. The reaction can then be characterized by the rate coefficient, k^+, which will be indicated by writing

$$A + A \xrightarrow{k^+} P$$

Often we are able to express the equations that determine the rate coefficients, k^+, in a natural way in terms of k^+/D. This suggests defining a reduced rate coefficient

$$y := \frac{k^+}{D} \tag{2}$$

In 2-d we have the special situation that y is dimensionless and most of the equations we are dealing with turn out to be independent of the diffusion coefficient, D, if expressed in terms of y. Analogously a dimensionless concentration variable, z, may be defined as

$$z := \rho R_{enc}^2 \tag{3}$$

Many relationships can be expressed in dimensionless form using the variables y and z. The actual values k^+ or ρ are obtained easily by multiplication of y or z with the actual diffusion coefficient, D, or the square of the encounter radius, R_{enc}, respectively. All concentrations, ρ, are expressed in 'particles per area', usually employing the unit $[1/nm^2]$.

2.2. Theoretical approaches

Here, we focus on the results of the various theoretical approaches for the DC 2-d reaction according to scheme (1) in the steady-state regime. Keizer obtains

$$y = \frac{\pi}{K_0(2\sqrt{yz})} \tag{4}$$

For a detailed derivation and discussion of this result see [12,13,19,20]. Note that Eq. (4) is an implicit equation which has to be solved numerically. $K_0(x)$ denotes McDonald's function of zeroth order and can be found in tables or as predefined function in various recent computer algebra software systems such as [21]. The quantities y and z are defined in Eq. (2) and Eq. (3). We emphasize that in contrast to the case of 3-d reactive processes in which Smoluchowski's approach gives a true constant, in 2-d the rate coefficient, k^+, is concentration dependent. The concentration dependence can be seen from Fig. 2; it illustrates the solution of Eq. (4) as a function of z, which can be converted to conventional units using the reference values $R_{enc} = \sqrt{\rho}/z = 1$ nm and $D = k^+/y = 5 \times 10^6$ nm^2/s. Notice that Eq. (4) has a solution up to a maximal value of $y_{Bif} \approx 0.038$. Indeed, Eq. (4) has two branches of solutions with

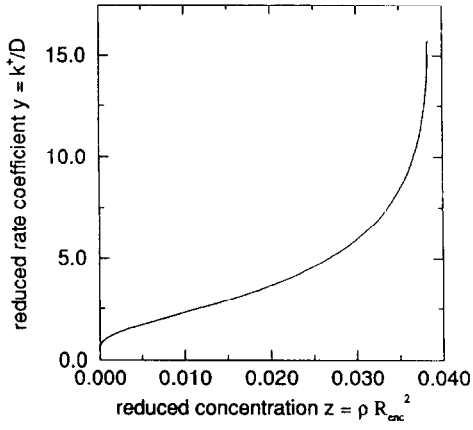

Fig. 2. Concentration dependence of the reduced rate coefficient, $y = k^+/D$, according to the implicit Eq. (4) in the case of an infinite membrane. Above a concentration of about $\rho = 0.0383/R_{enc}^2$, which is far below the close-packed density, $\rho_{cp} = 2/\sqrt{3}\,R_{enc}^2 \approx 1.155/R_{enc}^2$, Eq. (4) has no solution.

y_{Bif} as a bifurcation point. Only the lower branch, shown in Fig. 2, gives values which have physical meaning. Eq. (4) ceases to have a solution above a concentration of about $\rho = 0.0383/R_{enc}^2$, far below the close-packed density $\rho_{cp} \approx 1.155/R_{enc}^2$. The questions of how these findings should be understood and in which range of concentration Eq. (4) gives a good approximation will be considered below.

Hardt [8] has worked out a simple approach for rates of 2-d DC steady-state reactions according to the scheme

$$A + B \xrightarrow{k^+} P \tag{5}$$

Although she did not treat the case for identical particles explicitly, we can easily obtain the rate coefficient for reaction scheme (5) using her approach. According to Hardt's approach

$$V^+ = \frac{\rho_A}{\tau_A} + \frac{\rho_B}{\tau_B} \tag{6}$$

in which τ_A or τ_B are the mean diffusion times of A or B particles, respectively, till reaction occurs. For the mean diffusion time in the 2-d case, Hardt applies the approximative expression derived by Delbrück and Saffman [22]

$$\tau_j = \frac{b_j^2}{2D_j} \ln\left(\frac{b_j}{R_{enc}}\right) \tag{7}$$

with $j = A,B$ and b_A or b_B denoting the average areas available for A or B assuming cells containing a single fixed B or A, respectively. The b_A and b_B are defined by

$$\pi b_A^2 = \frac{1}{\rho_B}$$

$$\pi b_B^2 = \frac{1}{\rho_A} \tag{8}$$

Inserting the expression (7) and (8) into Eq. (6) gives

$$V^+ = 2\pi\rho_A \rho_B \times \left(\frac{D_A}{\ln\left(\frac{1}{R_{enc}\sqrt{\pi\rho_B}}\right)} + \frac{D_B}{\ln\left(\frac{1}{R_{enc}\sqrt{\pi\rho_A}}\right)} \right) \tag{9}$$

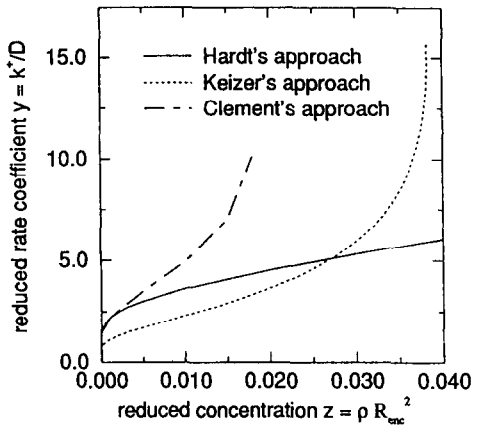

Fig. 3. Overview of the infinite membrane approaches for k^+/D of Hardt, Keizer, and Clément et al., according to the Eqs. (10), (4), and (18), respectively. Again, $y = k^+/D$ is plotted versus $z = \rho R_{enc}^2$.

The rate equation for identical particles is obtained from Eq. (9) by setting $D := D_A = D_B$, $\rho := \rho_A = \rho_B$, and dividing the right hand side of Eq. (9) by 2 so as not to count reaction events twice. This gives the reduced rate coefficient, $y = k^+/D$, in terms of the reduced concentration, $z = \rho R_{enc}^2$, as

$$y = -\frac{4\pi}{\ln(\pi z)} \tag{10}$$

Fig. 3 shows a plot of y versus z according to Eq. (10), which gives an interesting interpretation for πz. It can be interpreted as the probability that a particle meets another particle in the instant of its creation, e.g., as the result of a 'landing' process. For DC reactions, πz is then equal to the probability of an immediate reaction of a landing particle. It suggests the definition of the upper density limit as the close-packed density of disks having a radius of $r = R_{enc}$ with

$$\rho_{cp} := \frac{1}{2\sqrt{3}\,R_{enc}^2} = \frac{1}{4}\rho_{cp} \tag{11}$$

in contrast to ρ_{cp}, the close-packed density of disks with the actual particle radius of $r = R_{enc}/2$. Assuming a particle distribution with the density $\rho = \rho_{cp}$ in which the center to center particle distance is equal to the encounter radius, R_{enc}, we see that every particle creation will result in an immediate reaction. The corresponding rate coefficient will approach in-

finity. Depending on the particle distribution, the actual density limit in which every particle creation will result in a reaction lies somewhere between the two limits ρ_{cp} and ρ_{cp}. We have

$$\pi z \overset{\rho \to \rho_{cp}}{\to} \frac{\pi}{2\sqrt{3}} \approx 0.91 < 1 \tag{12}$$

implying that Eq. (10) is well defined and πz can be interpreted as a probability. The density limit, ρ_{cp}, is thus not relevant for DC reactions.

Clément et al. [18] proposed another approach for the description of the reaction kinetics of issue. Their approach recalls the approach of Keizer in that they approximate the infinite hierarchy of correlation functions, the exact set of equations for the description of a multiparticle system, by truncating them at the level of the pair correlation function. Their ansatz includes different types of particle sources necessary to maintain a steady-state regime. These sources take into account excluded volume effects. Clément et al. distinguish between an effective particle source Q, consisting of those particles, that succeed in landing at an empty site, and an overall constant particle source R. Two situations of net particle influx are considered. In the case in which a particle performing a landing attempt meets another particle within the encounter radius R_{enc}, Clément et al. [18] assume that both the landing particle and the occupying particle involved are annihilated. This situation is described by the relationship

$$Q = R(1 - 2z) \tag{13}$$

or they discard the landing particle, in which case

$$Q = R(1 - z) \tag{14}$$

In either case, at low concentrations and fixed encounter radius, R_{enc},

$$Q \approx R \tag{15}$$

Clément et al. showed that the effective reaction rate Q can be expressed in the unique general form

$$Q = \frac{4\pi D}{C_o + \frac{1}{2}\ln\left(\frac{\rho D}{R_{enc}^2 R}\right)}\rho^2 \tag{16}$$

depending on the net particle influx but being independent of the special form of the particle source. As discussed in detail in Ref. [18], $C_o = \ln 2/2 - \gamma \approx 0.116$ with γ being Euler's constant. Applying the approximation (16), we are able to define the reduced rate coefficient, y, by

$$y = \frac{k^+}{D} := \frac{Q}{2\rho^2 D} \tag{17}$$

and thus find the simple expression

$$y = \frac{2\pi}{0.116 - \frac{1}{2}\ln(2yz)} \tag{18}$$

Eq. (18) is again an implicit equation and has to be solved iteratively. Fig. 3 presents a solution of Eq. (18). As in the case of Keizer's approach, Eq. (18) has a solution only up to a certain reduced concentration, z_{crit}, even below the critical concentration of Keizer's approach presented by Eq. (4). A more detailed analysis which takes into consideration the excluded volume effects, presented by Eq. (13) and Eq. (14), will result in slightly steeper curves compared to the curve presented in Fig. 3. The solution of Eq. (18) ceases to exist below concentrations at which excluded volume effects will have a more pronounced impact. This implies that Eq. (15) is always valid. For low concentrations the solution of Eq. (18) approaches the solution of Hardt's approach, whereas Keizer's approach turns out to be a factor 1/2 smaller.

The case of a finite (spherical) membrane

Biomembranes are always of finite size and their surfaces are usually closed. In addition artificial model membranes are used in many cases in vesicular form of variable sizes for various experiments, e.g. Ref. [17]. It is therefore of interest to elucidate the influence of the system size on reaction rates.

Swartz and Peacock-López [23] applied Keizer's steady-state approach of $A + A \overset{k^+}{\to} P$ reactions to spherical surfaces. Their analysis, involving spherical harmonics, yields an implicit integral equation for $y = k^+/D$ that can be solved only numerically. In terms of the reduced variables y and $z = \rho R_{enc}^2$, this expression is

$$y = \pi\left(\int_0^\infty \frac{e^{-x/2}\cos\left((x/2)\left[16\frac{zy}{\alpha^2} - 1\right]^{1/2}\right)}{[1 - 2e^{-x}\cos\alpha + e^{-2x}]^{1/2}}\,dx\right)^{-1} \tag{19}$$

Notice that the implicit Eq. (19) depends not only on the diffusion coefficient, the reactant concentration, ρ, and the encounter radius, R_{enc}, but also on a quantity α which is related to the curvature of the sphere. As long as the particle size is small compared to the linear size of the sphere, it follows that $\alpha = R_{enc}/R_{ves}$, where R_{ves} is the size of the sphere or the outer radius of a vesicle. The complete expression for α is given in Eq. (19) of Ref. [23].

The plots in Fig. 4 are a numerically determined solution of Eq. (19). Keeping in mind the reference values in Section 2.1, the α-values correspond to vesicle radii, R_{ves}, of 15 nm and 30 nm. The infinite membrane case can be expressed by $\alpha = 0$, i.e. an infinite vesicle radius. It can be shown analytically that, for $\alpha \to 0$ and a fixed encounter radius, Eq. (19) changes into Eq. (4), which determines the reduced rate coefficient for unlimited membrane sizes [23]. The vesicle radii, R_{ves}, of 15 nm can be considered as the limit corresponding to the smallest possible size of a closed bilayer. Even then, only very small concentrations will result in an observable deviation of the reduced rate coefficient from the approximative values of the infinite membrane case (Fig. 4).

2.3. RW simulations

In the previous section we found that the theoretical approaches of Keizer, Hardt, and Clément et al. led to different solutions for the concentration dependent reduced rate coefficient, $y = k^+/D$, of the same reaction scheme.

As Fig. 3 indicates the density dependence of the solutions according to Keizer's and Clément's approach are similar. For increasing z both curves have a steep increase at low concentrations, a nearly linear middle part, and a steep increase at higher concentrations before a solution ceases to exist. Hardt's curve coincides with Clément's approach for low z and increases very slowly over the whole concentration range up to values somewhat above the lower density limit ρ_{cp}, where Eq. (10) has a singularity. At low concentrations, Keizer's solution for $y = k^+/D$ is about a factor 1/2 smaller than the solution of Hardt and Clément et al. This situation of different results for the same reaction scheme has to be clarified.

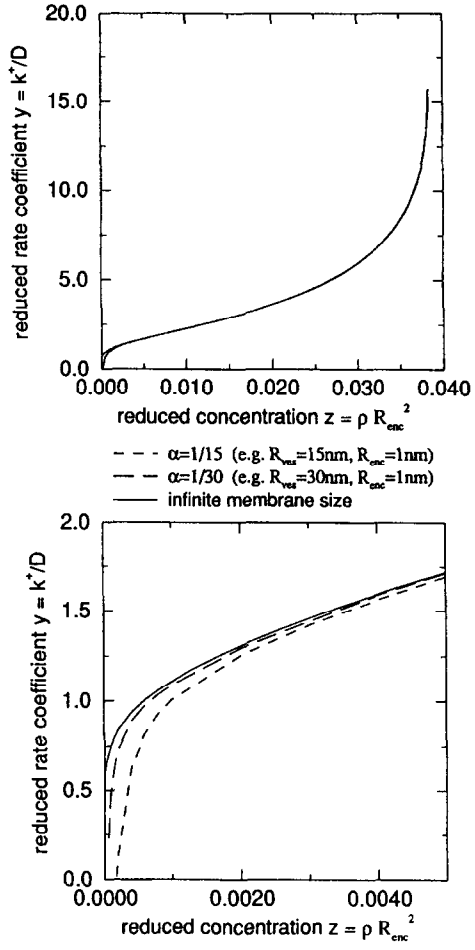

Fig. 4. Influence of membrane size on $y = k^+/D$ as calculated by a numerical evaluation of Eq. (19). The α-values used correspond to $R_{enc} = 1$ nm and vesicle radii of 15 nm, 30 nm, and ∞ (infinite membrane), respectively. An enlarged section of the low concentration region of the upper plot is shown below. The plots point out that only for low concentrations and small spheres an appreciable deviation of the k^+/D values from the values of the infinite membrane case can be observed. Only discrete values $z = k/\pi(\alpha/2)^2$, for discrete numbers $k = 2, 3, 4, \ldots$ of particles are allowed for the reduced concentration.

A method or an experiment has to be found which reflects the multiparticle properties of the diffusion reaction system under consideration in an appropriate manner. We stress that theoretical treatments of multiparticle systems are in general of an approximative nature. It is described exactly by a system of coupled equations involving in a hierarchical manner n equations for n correlation functions in the case of

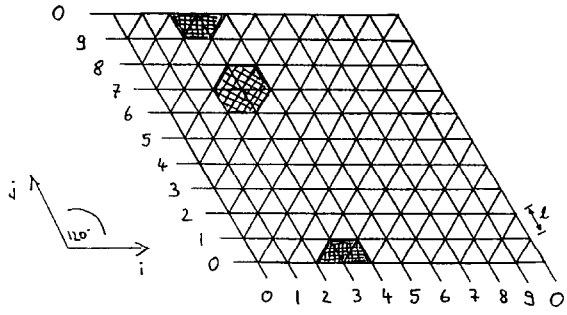

Fig. 5. Sketch of a 10×10 triangular lattice with periodic boundary conditions as used in varying sizes for the RW simulations. Two hexagonally shaped particles of diameter $R \triangleq 2$ lattice spacings are drawn in the lattice ($R_{enc} = 2l$).

an n-particles system [24]. Usually the hierarchy of correlation functions is truncated at the level of pair correlation functions as it is performed in the case of both Keizer's and Clément's approach. These requirements suggest the modeling of the reactive systems of interest as a RW simulation. Montroll [25–27] and Chandrasekhar [28] worked out the necessary theoretical underpinnings for a variety of different grid structures such as square, triangular, or hexagonal lattices. The structure of lipid bilayers gives the priority to a triangular lattice structure on which the solute particles will perform their RW by jumping from one site to one of its six nearest lattice points (Fig. 5). Additionally, disk shaped particles will be better approximated by hexagons on a triangular grid than by squares in the case of square lattices. RW simulations on triangular lattices have been applied by Pink [2] and Saxton [29] to elucidate, for example, the impact of mobile and immobile obstacles on protein diffusion in biomembranes.

Methods

Initially, a prescribed number N_A of particles A are distributed at random on a $N_g \times N_g$ triangular lattice with periodic boundary conditions with N_g denoting the number of line segments per side. Overlapping of particles is not allowed. For all performed simulations hexagons have been chosen as particles consisting of seven lattice points (Fig. 5). They represent and approximate the disk-shaped reactants A of an encounter radius of two lattice spacings. To check the influence of the hexagon size, some simulations are performed with larger hexagons and with one point particles also.

The simulation procedure starts by selecting one particle at random; it is then moved by equal chance one step in any of the six possible directions. If one of the six outer points of the hexagon overlaps an

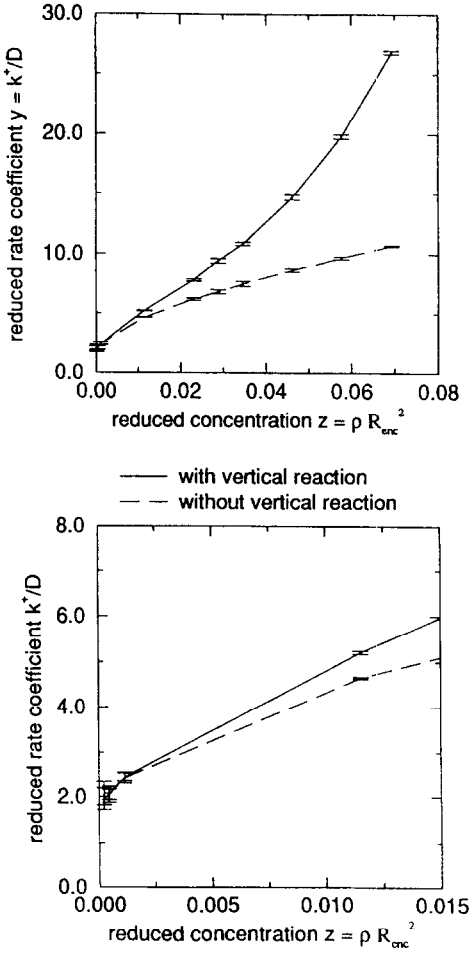

Fig. 6. Plot of $y = k^+/D$ versus $z = \rho R_{enc}^2$ determined by simulations with and without vertical reaction. For each data point the average k^+/D value and the pertinent std. dev. (error bars) of 10 simulations are calculated. The time lengths of the simulations vary between 10^4 MCS/particle for high concentrations up to 10^6 MCS/particle for low concentrations. The plot below shows an enlarged section of the low concentration region of the upper plot. The system sizes have been chosen large compared to the mean particle distance in order to approach infinite membrane sizes.

outer point of an adjacent A hexagon, instantaneous reaction occurs, meaning that both particles are annihilated. In the RW model the formation of an inert product according to scheme (1) is realized by a particle pair annihilation. To maintain a steady-state regime, the reacted particles are recreated at randomly chosen sites. These sites might be occupied by a particle, so that a particle overlapping would occur.

At this point we have the choice to proceed in two different ways: We first treat the particle overlap as a reactive encounter leading to an instantaneous annihilation of the particle on the lattice. This so called 'vertical reaction' (see e.g. [30]) is counted as one particle pair annihilation in the overall reaction balance. The two particles involved are redistributed, including the possibility of further vertical reactions. In a second set of simulations, vertical reaction is not allowed. Particles are placed randomly only at empty lattice sites.

Each time N_A particles have been randomly selected for performing the one-step random walk, the simulation time, t^*, is incremented by one. This ensures that on the average every particle is moved once during a time step, which is referred to as one Monte Carlo step per particle (MCS/particle). The total duration, t^*_{max}, of a simulation is given in MCS/particle.

The characteristic parameters of the RW on the triangular lattice are l, the lattice constant, which gives the distance of adjacent lattice points in nm; R^*_{enc}, the encounter 'radius' of the hexagons in lattice spacings; R_{enc}, the encounter 'radius' in nm defined by

$$R^*_{enc} = \frac{R_{enc}}{l} \tag{20}$$

and

$$\tau = \frac{l^2}{4D} \tag{21}$$

the mean square displacement of diffusing particles in two dimensions with D, the diffusion coefficient of the hexagonal particle and τ, the jumping time. The physical time, t, is

$$t = t^*\tau$$

The rate of the particle pair annihilation, V_{ani}, is given by

$$V_{ani} = k^+\rho_A^2$$

with ρ_A, the particle concentration of A's in particles/nm^2, and k^+, the rate coefficient. When we think of each annihilation as a creation of a product particle, P, which might be an encounter complex, we can identify

$$V_{ani} = \frac{\partial \rho_P}{\partial t}$$

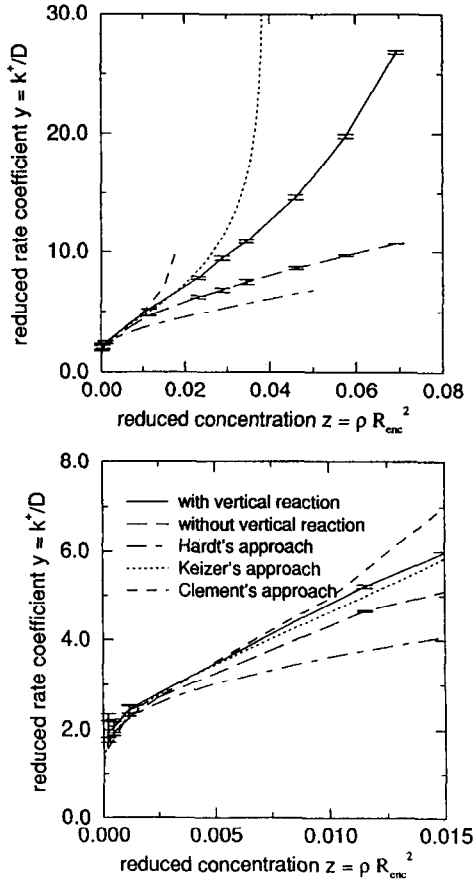

Fig. 7. Comparison of the numerically simulated k^+/D values as shown in Fig. 6 with the theoretically calculated values of Hardt's and Keizer's approach. The values of Keizer's modified approach have been used. The plot below shows an enlarged section of the low concentration region of the upper plot.

with ρ_P, the concentration of formed products, P. By discretizing the differential equation, we get

$$\frac{\Delta n_P}{\Delta t}\frac{1}{A_g} = k^+\left(\frac{N_A}{A_g}\right)^2 \tag{22}$$

with Δn_P, the counted number of particle pairs annihilated during the physical time interval, Δt. It is easily shown that the physical lattice area, A_g, satisfies the expression

$$A_g = \frac{\sqrt{3}}{2}\left(N_g \ell\right)^2 \tag{23}$$

Combining Eqs. (22) and (23) with

$$\Delta t = \Delta t^* \tau = \Delta t^* \frac{\ell^2}{4D}$$

give, after rearrangement, the dimensionless expression

$$y := \frac{k^+}{D} = 2\sqrt{3}\left(\frac{N_g}{N_A}\right)^2 \frac{\Delta n_p}{\Delta t^*}. \tag{24}$$

All programs are written in Ansi-C. The computations were performed on a cluster of Silicon Graphics Indigo workstations, except for the more time consuming simulations, which were performed on an Onyx workstation.

A crucial point of all Monte Carlo simulations is the choice of a well tested random number generator. System-supplied random number generators such as random in ANSI C are often of doubtful quality [31]. The random number generators in Press et al. [31], on the other hand, are well tested and have been widely accepted and used. Since some simulations call the random number generator more often than 10^9 times, the long period ($> 2 \times 10^{18}$) random number generator of l'Ecuyer with Bays–Durham shuffle and added safeguards [31] has been used.

Testing of the random walk programs

All simulation programs display the output as a graphic animation. After each time step, coloured dots indicate the actual position of each particle in a rectangular window. The animation provides a useful tool for an immediate checking of the correctness of the program.

Besides the usual permanent syntax checking, some further testing of the simulation program has been done. The mean square displacement of a single particle performing a random walk in one of the simulations has been determined. After a prescribed time-difference (e.g. $t^* = 50$ MCS/particle), the square of the Euclidian distance to the starting point was calculated. This procedure was repeated up to 1200 times. The averaged values are in good agreement with theory. The above values and a grid size of 500×500 gave a mean square displacement of about 50.125 lattice spacings whereas theory predicts 50 lattice spacings. This testing has been repeated with various grid sizes and time increments, and the outcomes have always been found to be in good agreement with the theoretically predicted value.

In a series of publications Montroll [25], Montroll and Weiss [26], and Montroll [27], develop a theory of random walkers on different lattice structures in the Euclidian dimensions 1-d, 2-d, and 3-d. In 2-d an exact theory for a variety of important properties of random walkers on various lattices has been described. For the concrete cases of square, triangular, and hexagonal 2-d lattice structures with periodic boundary conditions, approximations of the exact expressions for the mean first passage time of random walkers as a function of the linear lattice size, N_g, are derived [27].

In the following we apply this approach for triangular lattices in order to derive an exact expression of the reduced rate coefficient, y_{theory}, for a steady-

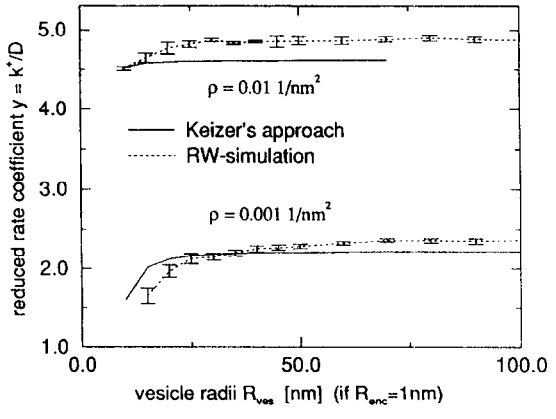

Fig. 8. The plot illustrates the dependence of the reduced rate coefficients y on the vesicle sizes for two different concentrations ρ due to the theoretical approach of Swartz and Peacock-López, according to the integral Eq. (19), and the RW simulations.

state concentration, ρ, corresponding to the situation in which two distinct one-point particles are distributed in a preassigned area, A. We choose one distinct site of the triangular lattice as the trap. Then $\langle n \rangle$ denotes the average number of steps for a one-point random walker to reach the fixed trap for the first time when the RWer starts from randomly chosen non-trap lattice sites. Montroll obtains for the mean first passage time $\langle n \rangle$ the expression [27]

$$\langle n \rangle = \left\{ c_1 N \ln N + c_2 N + c_3 + O\left(\frac{1}{N}\right) \right\} \frac{N}{N-1} \tag{25}$$

with $N \overset{Def}{=} N_g^2$ and the constants

$$c_1 = \frac{\sqrt{3}}{2\pi}, \quad c_2 = 0.235\,214\,021,$$

$$c_3 = -0.251\,407\,596$$

As a consequence of the relativity of motion, we see immediately that the situation of the lateral motion involving a mobile particle and an immobile sink is equivalent to the situation in which two particles jump in an alternate turn. Hence, in terms of the mean first passage time $\langle n \rangle$, we find the expression for the reduced rate coefficient for two random walking one-point particles with

$$y = \frac{k^+}{D} = 2\sqrt{3}\left(\frac{N_g}{N_A}\right)^2 = 2\sqrt{3}\,\frac{N_g^2}{4}\,\frac{1}{\left(\frac{\langle n \rangle}{2}\right)} \tag{26}$$

The last term holds as on average one particle pair is annihilated in a time interval of $\Delta t^* = \langle n \rangle / 2$. This is obvious as a total amount of two jumps for the two particles results in a time increment of one MCS/particle. Inserting the expression (25) in Eq. (26) gives after simple algebraic manipulations

$$y = \frac{\pi}{\frac{\pi}{\sqrt{3}} c_2 + \ln N_g} \tag{27}$$

for sufficiently large N_g.

For $N_g = 12$ we find a theoretical value according to Eq. (27) of

$$y_{\text{theory}} = 1.0790$$

whereas RW simulations with one-point particles, i.e. $R_{\text{enc}} = 0$ and $N_g = 12$, averaged over 10 runs having each a time limit of 10^6 MCS/particle yield

$$y_{\text{RW}} = 1.07221 \quad (\text{std. dev.: } 0.0115)$$

The agreement is additional evidence for the correctness of the RW simulations.

2.4. Results

In the first set of simulations, values of k^+/D were determined for different concentrations, either including or excluding vertical reactions. The lattice

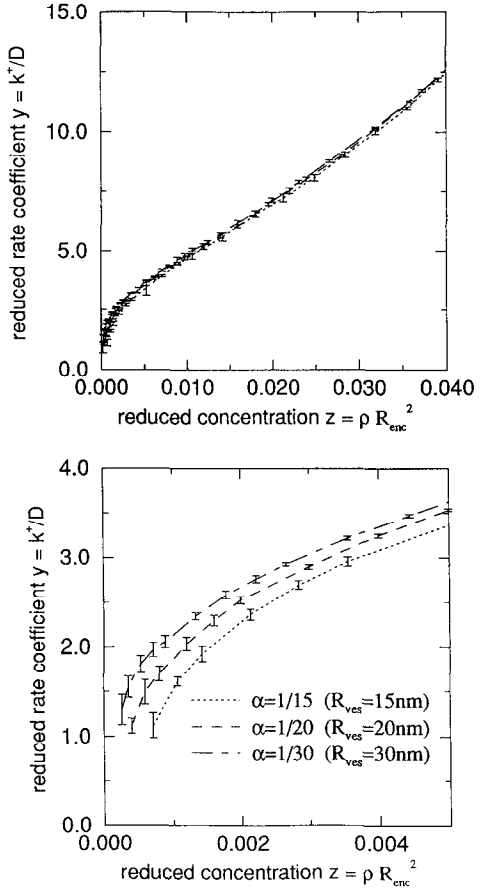

Fig. 9. Influence of membrane size on $y = k^+/D$ due to RW simulations. The indicated relative sizes $\alpha = R_{\text{enc}}/R_{\text{ves}}$ fit vesicles of the mentioned appropriate radii, if an encounter radius of $R_{\text{enc}} = 1$ nm is chosen. The plot below shows the enlarged low concentration region of the plot above. As in Fig. 8, z adopts only the discrete values $z = k/\pi(\alpha/2)^2$ for discrete numbers $k = 2, 3, 4, \ldots$ of particles. The curves should only guide the eyes.

size was chosen large compared to the mean particle distance. This was measured by the ratio between mean particle distance and lN_g, the linear system size, which is small even for the lowest particle concentrations (below 0.1). Fig. 6 shows a plot of $y = k^+/D$ versus $z = \rho R_{enc}^2$ determined by simulations with and without vertical reactions.

A typical concentration dependence of k^+/D can be read directly from Fig. 6 by dividing z by $R_{enc}^2 = 1\ nm^2$, the square of the reference encounter radius described in Section 2.1. It is obvious that for low reactant concentrations a vertical reaction has practically no influence on the reaction rate. Therefore both curves in Fig. 6 coincide for small concentrations ($z < 0.005$). Comparison of the theoretically calculated k^+/D of Section 2.2 with the numerically simulated k^+/D values as illustrated by Fig. 7 clearly shows good agreement of Hardt's approach with the simulation result for low concentrations. For higher concentrations (i.e. $z > 0.005$), Hardt's approach agrees qualitatively with the numerically simulated k^+/D values which excludes vertical reaction. Keizer's approach gives k^+/D values by a factor of $1/2$ smaller than the simulated values shown in Fig. 3. After multiplying the k^+/D values of Keizer's approach by two, there is nice agreement at low concentration and qualitative agreement with the values of the simulation that include vertical reactions at higher concentrations (Fig. 7).

The approach using Keizer's theory, as cited above, assumes a constant, non-fluctuating particle source for the maintenance of the steady-state regime. If fluctuations in the particle source are included, Molski and Keizer showed that the rate coefficient will increase by exactly a factor of two [32]. The reasons for this difference is unclear. However, a fluctuating particle source, as also realized in the simulations, is a more realistic assumption than a constant source. In the case of Keizer's theory, we will talk, henceforth, of the 'modified approach' when we think of the reduced rate coefficient multiplied by the factor of two. Fig. 7 shows the modified values of Keizer's approach.

Influence of membrane size on reaction rates

RW simulations were also performed for different grid sizes. Assuming an encounter radius of 1 nm, the chosen lattice sizes correspond to vesicle sizes of outer radii from 15 nm up to 100 nm. Fig. 8 shows both the numerically simulated and theoretically calculated k^+/D values for two fixed reactant concentrations of $\rho = 0.001\ 1/nm^2$ and $\rho = 0.01\ 1/nm^2$ as a function of vesicle size. The theoretical values based on Eq. (19) have been multiplied by the factor of two, as mentioned above. Note that the topologies of the reactive systems used in the RW simulations and in the theoretical calculation are similar but not identical. The periodic boundary condition used in the simulations is topologically equivalent to a torus, whereas the calculations of Peacock-López and

Table 1
Presentation of numerically simulated and theoretically determined y values for a various number of peptides, n_A, per vesicle for two sizes of SUVs. τ_{dimer} denotes the average time needed to form a dimer (or encounter complex). The index 'sim' or 'Keiz' indicates that the corresponding value has been determined by numerical simulation or Keizer's modified infinite membrane approach, respectively. R_{ves} denotes the vesicle radius and y_{sim}/y_{Keiz} gives a measure for the influence of the system size on the reaction rate coefficient. The presented values have been determined up to the limit of $\rho_A = 0.01\ 1/nm^2$, as discussed in the text

n_A	$R_{ves} = 15$ nm						$R_{ves} = 30$ nm					
	ρ_A [1/nm^2]	y_{sim}	τ_{sim} [μs]	y_{Keiz}	τ_{Keiz}	y_{sim}/y_{Keiz}	ρ_A [1/nm^2]	y_{sim}	τ_{sim} [μs]	y_{Keiz}	τ_{Keiz} [μs]	y_{sim}/y_{Keiz}
2	0.000707	1.12	126.2	2.07	68.2	0.54	0.000177	1.64	612.7	0.923	345.7	0.56
4	0.00141	1.93	18.3	2.40	14.7	0.80	0.000354	1.55	91.2	1.83	77.4	0.85
10	0.00354	2.96	1.9	3.07	1.84	0.96	0.000884	2.06	11.0	2.17	10.4	0.95
20	0.00707	3.95	0.36	3.95	0.36	1.00	0.00177	2.59	2.2	2.54	2.2	1.02
25	0.00884	4.41	0.21	4.36	0.21	1.01	0.00221	2.76	1.3	2.68	1.3	1.03
50	–	–	–	–	–	–	0.00442	3.47	0.26	3.30	0.27	1.05
100	–	–	–	–	–	–	0.00884	4.63	0.049	4.36	0.051	1.06
110	–	–	–	–	–	–	0.00973	4.76	0.039	4.56	0.041	1.04

Swartz are performed for spherical reactive systems. Both have in common that their reactive planes are closed, an essential feature of biomembranes.

Though the topologies of the two approaches are different, Figs. 9 and 8 in comparison to Fig. 4 show agreement of the theoretically simulated results. Only for small concentrations and small vesicle radii, does membrane size have any influence on the reaction rate.

3. Discussion

In summary, it is interesting that the simple approach of Hardt (Eq. (10)) does a reasonable job of describing DC reactive processes involving identical particles [8]. Especially in the low concentration limit ($z < 0.005$) we find nice agreement between her approach and the simulations and even for concentrations between $z = 0.005$ and $z = 0.01$ it gives a rough approximation to the rate coefficient. For $z > 0.01$ Hardt's approach leads to a lower estimate of the reaction rates, roughly approximating y for reactive processes in which 'landing' effects of particles are ignored.

The range of agreement of Keizer's modified approach with the simulation results for $z < 0.01$ is larger than for Hardt's approach. At $z \approx 0.01$ the influence of the 'landing' process to the overall reaction rate starts to become more prominent. For these concentrations Keizer's approach gives an approximation of the rate coefficient of reactive processes that includes reaction of 'landing' particles. Both approaches are complementary to each other since at higher concentrations they give lower and upper bounds for the rate coefficients of the DC reactive processes.

To clarify how these results can be applied to specific reactions in membranes, we use them to describe the example referred to in Section 2.1, i.e. DC steady-state dimerizations of disk shaped peptides ($R_{enc} = 1$ nm) distributed on spherically shaped vesicles. For concreteness we consider radii of $R_{ves} = 15$ nm and $R_{ves} = 30$ *nm*, corresponding to the size of SUVs used in various experimental approaches [15,17]. In order to compare more closely to experiment, we will use the number of peptide molecules per vesicle, n_A, instead of the number of particles per area as the unit of density. The frequency of formation of encounter complexes is then $V_{dimer} = 4\pi\dot{\rho}_{\overline{AA}}R_{ves}^2$, and

$$\tau_{dimer} = \frac{1}{v_{dimer}} = \frac{4\pi R_{ves}^2}{yDn_A^2} \tag{28}$$

is a measure of the average time period needed to form one dimer. Table 1nn presents the numerically simulated y values for the two vesicle sizes for various n_A. Additionally, for each set of parameters, Table 1 gives the reduced rate coefficient according to Keizer's modified infinite membrane approach. We immediately see that the DC reaction is a fast process, for which the τ_{dimer}-values are spread over a range of 4 orders of magnitudes. Even for steady-state concentrations as low as 2 peptides per vesicles, τ_{dimer} is of the order of tenths of milliseconds. The influence of n_A is most pronounced for $n_A = 2$. For both vesicle sizes the encounter rates are roughly one half of the rates belonging to the infinite reactive system with corresponding peptide concentrations of $\rho = 2/4\pi R_{ves}^2$. Above a value of approximately 10 particles per vesicle we do not find any pronounced influence of the system size. As Table 1 shows, the reduced rate coefficient can be calculated by applying Keizer's modofoed infinite membrane approach up to the concentration limit of $\rho_A = 0.01\ 1/nm^2$.

Acknowledgements

I thank G. Schwarz, J. Keizer, J. Wagner, and M. Saxton for helpful discussions, and F. Roesel for support in solving Eq. (19). Financial support from the Roche Research Foundation and the Freie Akademische Gesellschaft during my stay at the Institute of Theoretical Dynamics, UC Davis, is kindly acknowledged. I would like to thank Joel Keizer for his hospitability during my stay at the Institute of Theoretical Dynamics.

References

[1] S.J. Singer and Garth L. Nicolson, The fluid mosaic model of the structure of cell membranes, Science, 175 (1972) 720–731.

[2] D.A. Pink. Protein lateral movement in lipid bilayers, simula-

tion studies of its dependence upon protein concentration, Biochim. Biophys. Acta, 818 (1985) 200–204.
[3] M.J. Saxton, Lateral diffusion in an archipelago; the effect of mobile obstacles, Biophys. J., 52 (1987) 989–997.
[4] M.J. Saxton, Anomalous diffusion due to obstacles: A Monte Carlo study, Biophys. J., 66 (1994) 394–401.
[5] M. Delbrück and G. Adam, Reduction of dimensionality biological diffusion processes, in A. Rich and N. Davidson (Editors), Structural Chemistry and Molcular Biology, Freeman, San Francisco, 1968, p. 193.
[6] S.S. Gupte, E.-S. Wu, L. Hoechli, M. Hoechli, K. Jacobson, A.E. Sowvers and C. Hackenbrock, Relationship between lateral diffusion, collision frequency, and electron transfer of mitochondrial inner membrane oxidation–reduction components, Proc. Natl. Acad. Sci. USA, 81 (1984) 2606–2610.
[7] S.S. Gupte and C. Hackenbrock, The role of cytochrome *c* diffusion in mitochondrial electron transport, J. Biol. Chem., 263 (11) (1988) 5248–5253.
[8] S.L. Hardt, Rates of diffusion controlled reactions in one-, two-and three-dimensions, Biophys. Chem., 10 (1979) 239–243.
[9] J. Keizer, J. Ramirez and E. Peacock-López, The effect of diffusion on the binding of membrane-bound receptors to coated pits, Biophys. J., 47 (1985) 79–88.
[10] E. Peacock-López and J.A. Ramirez, The effect of diffusion on the trapping of membrane-bound receptors by localized coated pits, Biophys. Chem., 25 (1986) 117–125.
[11] M.W. Swartz and E. Peacock-López, A theoretical model of LDL-receptor trapping on a spherical cell, Biophys. Chem., 44 (1992) 1–9.
[12] J. Keizer, Statistical Thermodynamics of Nonequilibrium Processes, Springer Verlag, Berlin, 1987.
[13] J. Keizer, Theory of rapid bimolecular reactions in solution and in membranes, Acc. Chem. Res., 18 (1985) 235–241.
[14] G. Schwarz, S. Stankowski and V. Rizzo, Thermodynamic analysis of incorporation and aggregation in a membrane: Application to the pore-forming peptide alamethicin, Biochem. Biophys. Acta, 86 (1986) 141–151.
[15] G. Schwarz, H. Gerke, V. Rizzo and S. Stankowski, Incorporation kinetics in a membrane, studied with the pore-forming peptide alamethicin, Biophys. J., 52 (1987) 685–692.
[16] G. Schwarz and G. Beschiaschvili, Thermodynamic and kinetic studies on the association of melittin with a phospholipid bilayer, Biochem. Biophys. Acta, 979 (1989) 82–90.
[17] G. Schwarz and C.H. Robert, Pore formation kinetics in membranes, determined from the release of marker molecules out of liposomes or cells, Biophys. J., 58 (1990) 577–583.
[18] E. Clément, L.M. Sander and R. Kopelman, Steady-state diffusion-controlled $A + A \rightarrow 0$ reaction in Euclidean and fractal dimensions: Rate laws and particle self-orderin, Phys. Rev. A, 39 (12) (1989) 6472–6477.
[19] J. Keizer, Nonequilibrium statistical thermodynamics and the effect of diffusion on chemical reaction rates, J. Phys. Chem., 86 (1982) 5052–5067.
[20] J. Keizer, Effect of diffusion on reaction rates in solution and in membranes, J. Phys. Chem., 85 (1981) 940–941.
[21] Maple V Release 2, Waterloo Maple Software, 1993.
[22] P.G. Saffman and M. Delbrück, Brownian motion in biological membranes, Proc. Nat. Acad. Sci. USA, 72 (1975) 3111–3113.
[23] M.W. Swartz and E. Peacock-López, Two-dimensional reactive systems: Rapid bimolecular processes on spherical surfaces, J. Chem. Phys., 95 (4) (1991) 2727–2731.
[24] T.L. Hill, Statistical Mechanics, Dover Publications, 1957.
[25] E.W. Montroll, Random walks on lattices, Proc. Symp. Appl. Math., 16 (1964) 193.
[26] E.W. Montroll and G.H. Weiss, Random walks on lattices —II, J. Math. Phys., 6 (2) (1964) 167.
[27] E.W. Montroll, Random walks on lattices —III. Calculation of first-passage times with application to exciton trapping in photosynthetic units, J. Math. Phys., 10 (4) (1968) 753.
[28] S. Chandrasekhar, Stochastic problems in physics and astronomy, in N. Wax (Editor), Noise and Stochastic Processes, Dover Publications, 1954, pp. 3–92.
[29] M.J. Saxton, Lateral diffusion and aggregation; a Monte Carlo study, Biophys. J., 61 (1992) 119–128.
[30] L.A. Harmon, L. Li, L.W. Anacker and R. Kopelman, Segregation measures for diffusion-controlled $a + b$ reactions, Chem. Phys. Lett., 163 (6) (1989) 463–468.
[31] W.H. Press, S.A. Teukolsky, W.T. Vetterling and B.P. Flannery, Numerical Recipes in C, Cambridge University Press, Cambridge, 2nd edition, 1992.
[32] A. Molski and J. Keizer, External noise, density fluctuations, and divergences in steady-state reaction–diffusion systems, J. Chem. Phys., 9 (1) (1991) 574–581.